Morel, D.L., Morell, K.D., Keller, E.A., and Rittenour, T.M., 2021, Quaternary chronology and rock uplift recorded by marine terraces, Gaviota coast, Santa Barbara County, California, USA: GSA Bulletin, https://doi.org/10.1130/B35609.1.

Supplemental Material

TABLE S1. RADIOCARBON SAMPLE LAB NUMBERS AND SITE COORDINATES

TABLE S2. LUMINESCENCE SAMPLE LAB NUMBERS AND SITE COORDINATES

Figure S1. Radial plots of IRSL age distributions. The number of aliquots accepted and measured (in parentheses) and the over-dispersion (OD, scatter) in the data are provided for each sample.

Figure S2. Luminescence properties of quartz samples. Plots are produced from 10 aliquots from each sample that passed rejection criteria. Data in each plot are shown from the same 10 aliquots. Plotted data include (from left to right for each sample) a dose-response curve, a plot of the first 5 s of the signal decay curves, and a histogram of the average Fast Ratios from the same signal decay curves. Note that Duncan and Duller (2011) suggest that samples with Fast Ratios > 20 are interpreted to be dominated by the fast component needed for accurate OSL dating. The apparent OSL age, number of aliquots used to calculate that apparent age, the number of aliquots analyzed are reported in parentheses, the over-dispersion (OD) of the data and the character of the equivalent dose distribution are also included.

Figure S3. Comparison of apparent OSL ages with fading corrected IRSL ages. Notice that quartz OSL results produce younger apparent ages than the IRSL results, except sample USU-2596 which had the highest average Fast Ratio, indicating that most aliquots in this sample were dominated by the Fast-decay component needed for accurate OSL age results. Results for sample USU-2660 are outside the 2se error for the apparent OSL and IRSL age estimates, but plot within the 10% uncertainty range of the 1:1 line. Fading corrected IRSL ages are interpreted to be more accurate from this study area based on these results and the weak fast-decay.

Figure S4. Luminescence properties of feldspar samples. Plots are produced from 10 aliquots from each sample that passed rejection criteria. Data in each plot are shown from the same 10 aliquots. Plotted data include a dose-response curve and a plot of the signal decay curves for the natural luminescence signals. Full distributions of equivalent dose (De) values are presented in Figure S1. Table 2 in the main text provides the fading corrected IRSL ages for each sample.

Text. Luminescence methods

TABLE S1. RADIOCARBON SAMPLE LAB NUMBERS AND SITE COORDINATES

Site ID	Site location	Lab ID	Lat (˚N)	Long (˚W)
COJ 1	Cojo Bay 1	192598	34.44950	-120.42400
COJ 2	Cojo Bay 2	192599	34.44950	-120.42400
WGV 2	West Gaviota Canyon 2	192597	34.46876	-120.24541
WGV	West Gaviota Canyon	191138	34.46986	-120.23647
WLV 1	West Las Varas Canyon 1	192594	34.44647	-119.97463
WLV 2	West Las Varas Canyon 2	191139	34.44647	-119.97463
WLV 3	*West Las Varas Canyon 3*	192595	34.44647	-119.97463
ENP	East Naples Point	192593	34.43530	-119.95427
EBC 1	East Bell Canyon 1	192591	34.42673	-119.90907
EBC 2	East Bell Canyon 2	192592	34.42673	-119.90907
IV 1	Isla Vista 1	192596	34.40938	-119.87068
IV 2	Isla Vista 2	192590	34.40938	-119.87068

TABLE S2. LUMINESCENCE SAMPLE LAB NUMBERS AND SITE COORDINATES

Site ID	Site location	Lab ID	Lat (˚N)	Long (˚W)
WSAG_osl1	West San Agustin Beach 1	USU-2661	34.45750	-120.35961
WSAG_osl2	West San Agustin Beach 2	USU-2662	34.45764	-120.35849
EAC_osl	East Alegria Canyon	USU-2660	34.46890	-120.26965
WEC_osl	West El Capitan	USU-2599	34.46106	-120.02977
WLV_osl	West Las Varas Canyon	USU-2598	34.44640	-119.97441
WNP_osl	West Naples Point	USU-2597	34.43627	-119.95700
ENP_osl1	East Naples Point 1	USU-2595	34.43547	-119.95453
ENP_osl2	East Naples Point 2	USU-2596	34.43547	-119.95453

LUMINESCENCE METHODS

Eight sediment samples were processed and analyzed at Utah State University Luminescence Laboratory in North Logan, Utah for infrared stimulated luminescence (IRSL) dating of feldspathic sand (Wintle, 1997). Samples were opened under dim amber light (~590 nm) and potentially light-exposed material from the outer ends of tubes was removed and discarded prior to further processing. The remaining sediment was then wet sieved to a target grain size range between 125 and 250 μm. Target ranges were treated with 10% hydrochloric acid and bleach/hydrogen peroxide to dissolve carbonates and organic material, respectively. Feldspar grains were twice separated from heavy minerals using sequential 2.7 g/cm^3 and 2.58 g/cm^3 density sodium polytungstate solutions and dried at room temperature (Wintle, 1997). All ages reported in the text are from IRSL dating of potassium feldspar, however we also report preliminary optically stimulated luminescence (OSL) results from quartz grains that were isolated and etched with 58% HF (see below).

Samples for dose-rate determination were collected from a 30 cm radius area surrounding the sample tube. Sediments were homogenized and representative samples were analyzed for radioisotope concentration using ICP-MS and ICP-AES techniques. These concentration values were converted to dose rate following the conversion factors of Guérin et al. (2011) and beta attenuation values of Brennan (2003). For the IRSL ages, the beta dose included contribution from 12.5% internal potassium (Huntley and Baril, 1997) and 400 ppm Rb (Huntley and Hancock, 2001) and an a-value of 0.086 (Rees-Jones, 1995). Contribution of cosmic radiation to the dose rate was calculated using sample depth, elevation and latitude/longitude following Prescott and Hutton (1994). Total dose rates were calculated based on water content, radioisotope concentrations, and cosmic contribution (Adamiec and Aitken, 1998; Aitken, 1998). See Table 3 in the main text.

Luminescence measurements on potassium feldspar following the IRSL single-aliquot regenerative dose (SAR) method of Wallinga et al. (2000) on 2-mm aliquots (~20–50 grains per disk). Infrared measurements were performed on Risø TL/OSL Model DA-20 readers with infrared light-emitting diodes (LEDs) (870 ± 40 nm) and reader dose rates of 0.10–0.11 Gy/sec from a decaying ^{90}Sr beta source (Bøtter-Jensen et al., 2003). The luminescence signal was measured through a blue filter pack of 2-mm and 4-mm thick filters (BG-39 and Corning 7–39, respectively) over 100 seconds (250 channels) at 50 °C with LED diodes at 85% power (~120 mW/cm^2). The resultant signal was calculated by subtracting the average of the last 10 seconds (chnls 225–250; background signal) from the first 0.8 seconds (chnls 1–2; peak signal) of the signal decay curve. Preheat conditions prior to natural, regenerative and test dose signals were at 250 °C held for 60 seconds (Blair et al., 2005). Dose response curves were fit within saturating-exponential and saturating-exponential plus linear fits to calculate equivalent dose (D_E) values.

The IRSL ages were calculated by correcting individual D_E measurements for fading (loss of signal with time, g_{2days} %/decade) using the method of Auclair et al. (2003) and the age correction model of Huntley and Lamothe (2001). Cumulative D_E and IRSL age values were calculated using the Central Age Model (CAM) of Galbraith and Roberts (2012). Aliquots were rejected if recycled (repeated) doses were >10% of unity, produced >10% of signal in the zero-dose step (recuperation) or if they had a natural D_E value greater than the highest regenerative dose given. Errors on D_E and age estimates are reported at 2-sigma standard error and include errors related to instrument calibration, dose rate and equivalent dose calculations, and were

calculated in quadrature using the methods of Aitken and Alldred (1972) and Guérin et al. (2011). Fading-corrected IRSL age distributions are shown in Figure S1.

Preliminary quartz OSL results were analyzed following the SAR method of Murray and Wintle (2000) on small-aliquots (2 mm diameter, ~20–50 grains per disk) of fine quartz sand (150–250 μm). Optical measurements were performed on Risø TL/OSL Model DA-20 readers, with stimulation by blue-green light emitting diodes (LED) (470 ± 30 nm) and the luminescence signal was detected through 7.5-mm UV filters (U-340) over 40 seconds (250 channels) at 125ºC with LED diodes at 90% power (36–45 mW/cm^2) at 125 °C over 40–50 s. Preheat temperatures prior to natural and regenerative dose measurements were 240 ºC and cutheat measurements before test dose measurement were at 160 ºC. Luminescence signals were calculated following the early background method (EBG, Cunningham and Wallinga, 2010) to enhance the signal from the fast decaying OSL component that is needed for accurate OSL age calculation. Signal responses to natural and laboratory doses were calculated as the average of an intermediate signal (1.6–2.4 s) subtracted from the sum of first 0.7 seconds of the OSL decay signal.

The quartz luminescence signals show decay rates and weak contribution of the fast-decaying component of the signal, essential for accurate quartz OSL results (Wintle and Murray, 2006). Average 'Fast ratio' values for aliquots that passed rejection criteria (based on >10% recuperation of the zero-dose step and recycling ratios of repeat points >10% of unity) range from 9 to 24 (Figure S2) and indicate that signals from most of the aliquots were not dominated by the fast-decay component (Durcan and Duller, 2011). One sample (USU-2596) had an average Fast ratio of 38.8, suggesting that at least some aliquots from this sample have suitable quartz signals for OSL dating. Figure S3 shows a comparison of the apparent quartz OSL ages and fading corrected feldspar IRSL ages from the same samples. Results of this comparison indicate that despite the use of the use of the EBG method of signal selection, the quartz OSL results produced younger ages than the feldspar IRSL ages in all cases except one. Sample USU-2596 produced OSL results within error of the IRSL age, this sample had the highest Fast ratio value (38.8) indicating the quartz OSL signal is dominated by the Fast decay component needed for accurate OSL dating. Sample USU-2660 produced an apparent OSL age that was slightly outside the 2-sigma error on the fading corrected IRSL age, but within 10% of the 1:1 unity line. This sample had the second highest Fast ratio value (24.1). Durcan and Duller (2011) suggest that quartz signals with a Fast Ratio >20 are dominated by the fast-decay component are preferred for dating.

We interpret the fading corrected feldspar IRSL results as the most accurate due to the weak fast-decay signals in the quartz OSL and resultant age underestimation in the apparent quartz ages.

IRSL Age Radial Plots

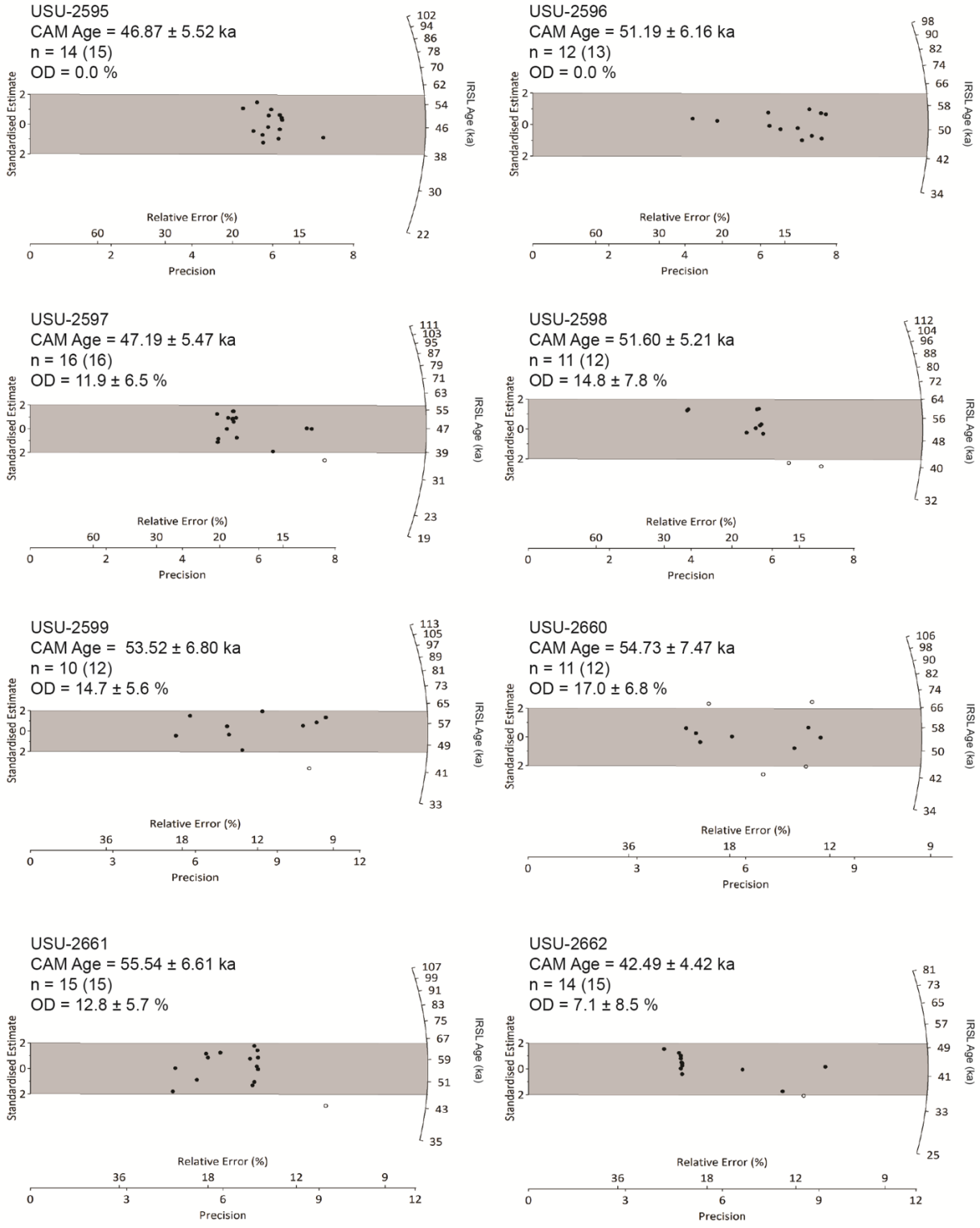

Figure S1. Radial plots of IRSL age distributions. The number of aliquots accepted and measured (in parentheses) and the over-dispersion (OD, scatter) in the data are provided for each sample.

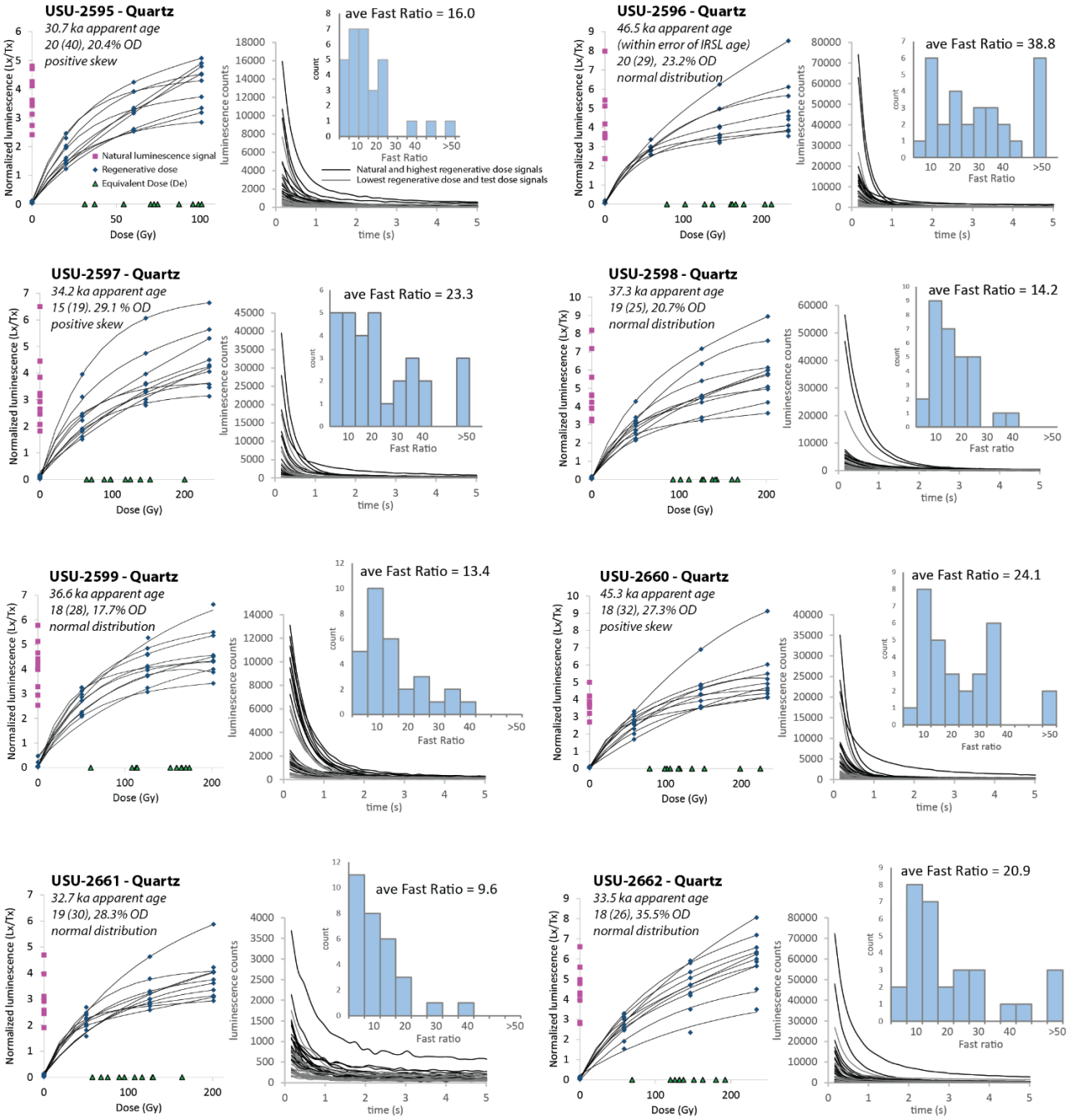

Figure S2. Luminescence properties of quartz samples. Plots are produced from 10 aliquots from each sample that passed rejection criteria. Data in each plot are shown from the same 10 aliquots. Plotted data include (from left to right for each sample) a dose-response curve, a plot of the first 5 s of the signal decay curves, and a histogram of the average Fast Ratios from the same signal decay curves. Note that Duncan and Duller (2011) suggest that samples with Fast Ratios > 20 are interpreted to be dominated by the fast component needed for accurate OSL dating. The apparent OSL age, number of aliquots used to calculate that apparent age, the number of aliquots analyzed are reported in parentheses, the over-dispersion (OD) of the data and the character of the equivalent dose distribution are also included.

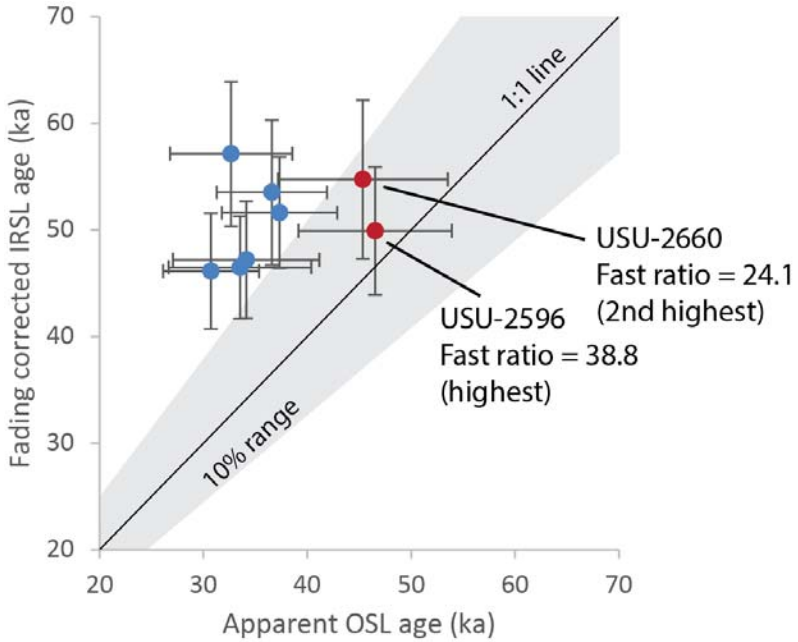

Figure S3. Comparison of apparent OSL ages with fading corrected IRSL ages. Notice that quartz OSL results produce younger apparent ages than the IRSL results, except sample USU-2596 which had the highest average Fast Ratio, indicating that most aliquots in this sample were dominated by the Fast-decay component needed for accurate OSL age results. Results for sample USU-2660 are outside the 2se error for the apparent OSL and IRSL age estimates, but plot within the 10% uncertainty range of the 1:1 line. Fading corrected IRSL ages are interpreted to be more accurate from this study area based on these results and the weak fast-decay.

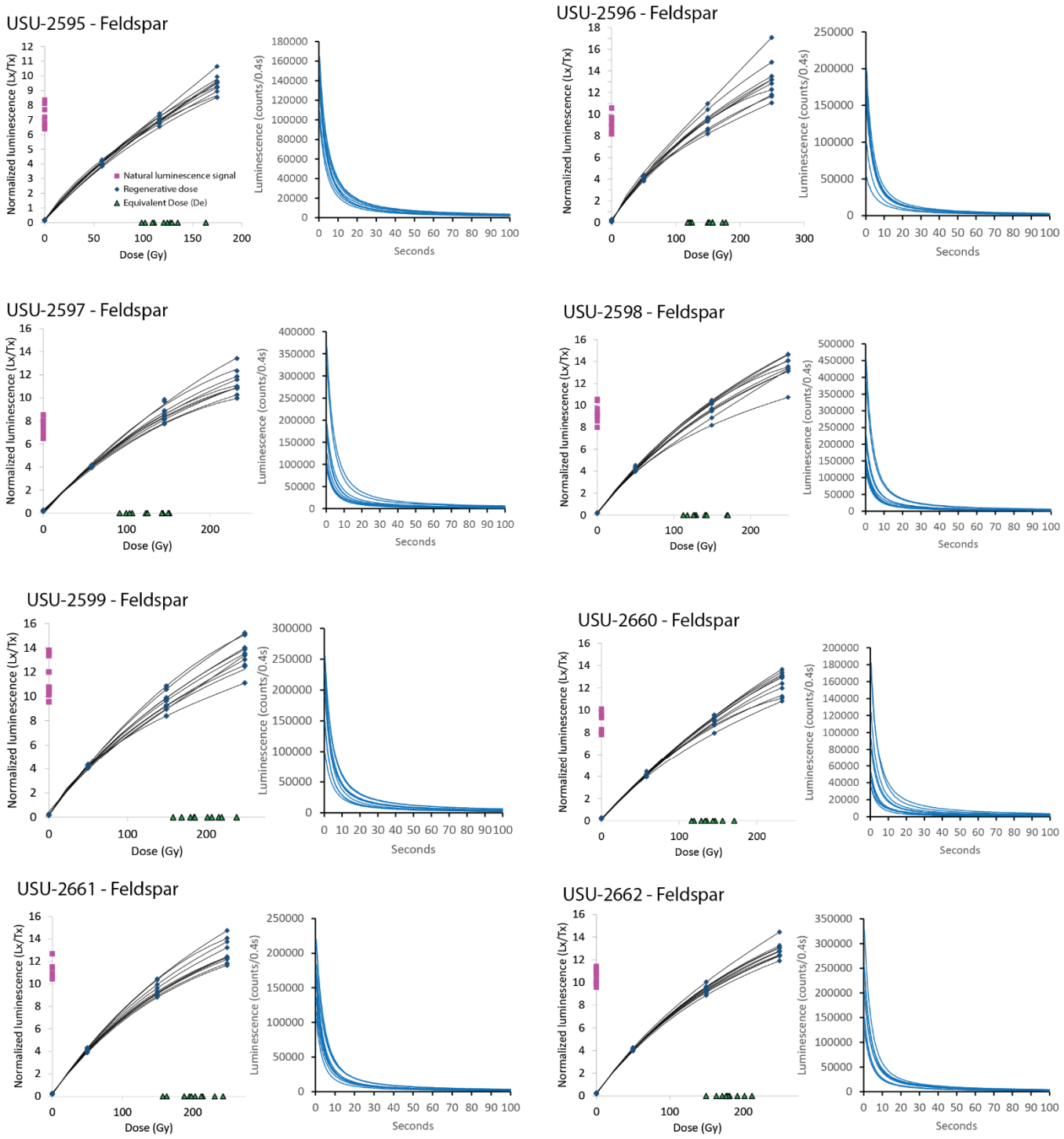

Figure S4. Luminescence properties of feldspar samples. Plots are produced from 10 aliquots from each sample that passed rejection criteria. Data in each plot are shown from the same 10 aliquots. Plotted data include a dose-response curve and a plot of the signal decay curves for the natural luminescence signals. Full distributions of equivalent dose (De) values are presented in Figure S1. Table 2 in the main text provides the fading corrected IRSL ages for each sample.

REFERENCES CITED

Adamiec, G., and Aitken, M.J., 1998, Dose-rate conversion factors: update: Ancient TL, v. 16, no. 2, p. 37–50.

Aitken, M.J., and Alldred, J.C., 1972, The assessment of error limits in thermoluminescene dating: Archaeometry, v. 14, p. 257–267, https://doi.org/10.1111/j.1475-4754.1972.tb00068.x.

Aitken, M.J., 1998: An Introduction to Optical Dating: The dating of Quaternary sediments by the use of photon-stimulated luminescence: New York, Oxford University Press, 267 p.

Auclair, M., Lamothe, M., and Huot, S., 2003, Measurement of anomalous fading for feldspar IRSL using SAR: Radiation Measurements, v. 37, p. 487–492, https://doi.org/10.1016/S1350-4487(03)00018-0.

Blair, M., Yukihara, E.G., and McKeever, S.W.S., 2005, Experiences with single-aliquot OSL procedures using coarse-grain feldspars: Radiation Measurements, v. 39, p. 361–374, https://doi.org/10.1016/j.radmeas.2004.05.008.

Bøtter-Jensen, L., Andersen, C.E., Duller, G.A.T., and Murray, A.S., 2003, Developments in radiation, stimulation and observation facilities in luminescence measurements: Radiation Measurements, v. 37, p. 535–541, https://doi.org/10.1016/S1350-4487(03)00020-9.

Brennan, B.J., 2003, Beta doses to spherical grains: Radiation Measurements, v. 37, no. 4–5, p. 299–303, https://doi.org/10.1016/S1350-4487(03)00011-8.

Cunningham, A.C., and Wallinga, J., 2010, Selection of integration time intervals for quartz OSL decay curves: Quaternary Geochronology, v. 5, no. 6, p. 657–666, https://doi.org/10.1016/j.quageo.2010.08.004.

Durcan, J.A., and Duller G.A, 2011, The fast ratio: a rapid measure for testing the dominance of the fast component in the initial OSL signal from quartz: Radiation Measurements. v. 46, no. 10, p. 1065-1072.

Galbraith, R.F., and Roberts, R.G., 2012, Statistical aspects of equivalent dose and error calculation and display in OSL dating: An Overview and some recommendations: Quaternary Geochronology, v. 11, p. 1–27, https://doi.org/10.1016/j.quageo.2012.04.020.

Guérin, G., Mercier, N., and Adamiec, G., 2011, Dose-rate conversion factors: update: Ancient TL, v. 29, p. 5–8.

Huntley, D.J., and Baril, M.R., 1997, The K content of the K-feldspars being measured in optical dating or in the thermoluminescence dating: Ancient TL, v. 15, no. 1, p. 11–13.

Huntley, D.J., and Hancock, R.G.V., 2001, The Rb contents of the K-feldspar grains being measured in optical dating: Ancient TL, v. 19, no. 2, p. 43–46.

Huntley, D.J., and Lamothe, M., 2001, Ubiquity of anomalous fading in K-feldspars and the measurement and correction for it in optical dating: Canadian Journal of Earth Sciences, v. 38, p. 1093–1106, https://doi.org/10.1139/e01-013.

Murray, A.S., and Wintle, A.G., 2000, Luminescence dating of quartz using an improved single- aliquot regenerative-dose protocol: Radiation Measurements, v. 32, p. 57–73, https://doi.org/10.1016/S1350-4487(99)00253-X.

Prescott, J.R., and Hutton, J.T., 1994, Cosmic ray contributions to dose rates for luminescence and ESR dating: Radiation Measurements, v. 23, p. 497–500, https://doi.org/10.1016/1350-4487(94)90086-8.

Rees-Jones, J., 1995, Optical dating of young sediments using fine-grain quartz: Ancient TL, v. 13, p. 9–14.

Wallinga, J., Murray, A., and Wintle, A., 2000, The single-aliquot regenerative-dose (SAR) protocol applied to coarse-grain feldspar: Radiation Measurements, v. 32, p. 529–533, https://doi.org/10.1016/S1350-4487(00)00091-3.

Wintle, A.G., 1997, Luminescence Dating: Laboratory Procedures and Protocols: Radiation Measurements, v. 27, p. 769–817, https://doi.org/10.1016/S1350-4487(97)00220-5.

Wintle A.G. and Murray A.S., 2006, A review of quartz optically stimulated luminescence characteristics and their relevance in single-aliquot regeneration dating protocols: Radiation measurements, v. 41, p. 369-391.